IOP Conference Series: Materials Science and Engineering

PAPER • OPEN ACCESS

Shear strength enhancement of reinforced self-compacting concrete box T-beams with different walled webs thickness using CFRP strips

To cite this article: Ali Hameed Aziz *et al* 2020 *IOP Conf. Ser.: Mater. Sci. Eng.* **737** 012029

View the article online for updates and enhancements.

You may also like

- Study on the destructive test of T-beam strengthened by external prestressing
Junyan Wu, Xiujuan Jiang and Laiyong Wang

- Shear Strengthening of T-Section RC Beams Using Double-Side Externally Bonded CFRP
Hazem Alfarra, Mohamed Maalej and Samer Barakat

- Strengthening of reactive powder concrete T-beams with openings
M B Abdulrahman and H M Rashid

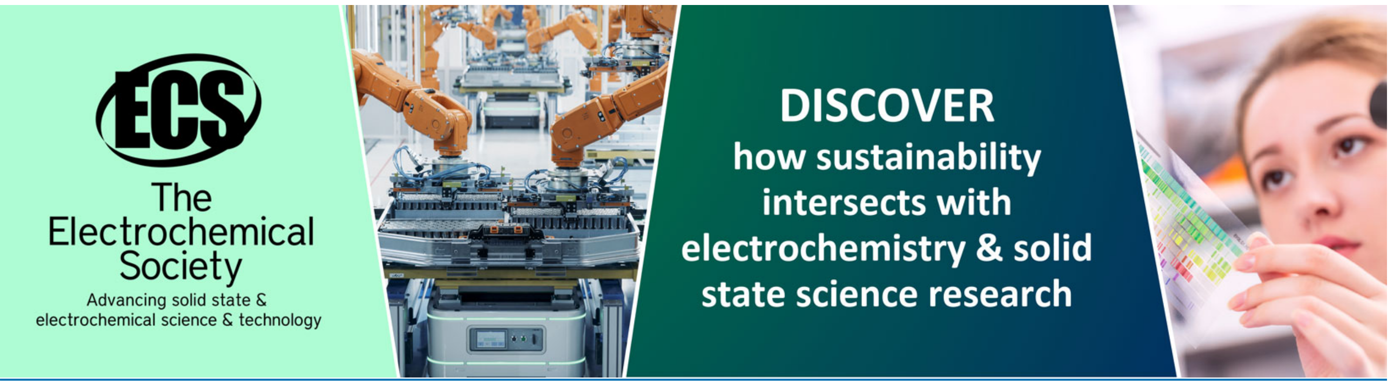

This content was downloaded from IP address 3.14.70.203 on 26/04/2024 at 16:18

IOP Conf. Series: Materials Science and Engineering **737** (2020) 012029 doi:10.1088/1757-899X/737/1/012029

Shear strength enhancement of reinforced self-compacting concrete box T-beams with different walled webs thickness using CFRP strips

Ali Hameed Aziz[1], Mutaz Kahdom Madhloom[1] and Muhammad Ali Jasem[1]

[1]College of Engineering-Mustansiriayah University-Baghdad-Iraq

E-mail: alihaziz@uomustansiriyah.edu.iq

Abstract. This paper deals with the effect of walled webs thickness variation and strengthening by CFRP strips on structural performance of reinforced self-compacting concrete (SCC) box T-beams subjected to shear loads. Eight reinforced SCC beam specimens have a dimension of (1500x200x300mm) for length; width and height, respectively were poured and tested. Three variables were adopted in the present study, section type (box or solid), web thickness (50mm, 62.5mm, 75mm, and 200mm) and with or without strengthening by CFRP. Experimental results show that the increase of the wall web thickness leads to increase the ultimate strength by about (17%-38%); while the strengthening of beams using CFRP strips led to increasing in ultimate capacity by about (75%-111%). All tested beams were analyzed by finite element method using ANSYS software. Also, a parametric study was performed based on two variables, concrete compressive strength, and the strengthening by prestressing forces. It was observed there is a simulation between the finite element analysis and the experimental results of about (102%) for ultimate capacity. Also, the increase of concrete compressive strength to (50MPa) leads to increase in ultimate load capacity about (11-17%), while the ultimate capacity increased for about (78-82%) when the beams were prestressed.

1. Introduction

Box beams are referred to as thin-walled structures because of their cross-sectional dimensions. The closed box section has high tensile stiffness, which ensures good transverse distribution of eccentric loads. As the box section has a high bending stiffness, this leads to efficient use of the complete cross-section. However, the prediction of the response of box beam bridges involves many difficulties caused by the complex interaction of the individual structural effects [1]. A box girder structure consists of top and bottom flanges connected by vertical or inclined webs to form a cellular section. It is one of the most popular forms of highway bridges; primarily because of the high flexural and torsion rigidities. The use of box beams in highway-bridge construction has proven to be a very efficient structural solution [2].

The shear failure has different characters, as compared to bending, in which the former is more brittle and often occurs without any forewarning. One of the techniques used to the strengthening of the existing reinforced concrete members involves externally bonding CFRP composite materials by means of epoxy adhesives. This technique improves the structural performance of a member under ultimate load and service load [3, 4, 5]. When the Tee beams (T-section beams) subjected to shear stresses, the thin vertical part of the beam (i. e. webs) will resist these stresses. New researches on T-beams show that the concrete flanges provide a certain level of shear resistance above a certain width [6, 7]. But the current codes of practice such as ACI 318-M14 [8], do not include an increase in shear strength resulting from the inclusion of a flange. Several researches are interested in box beams under

Content from this work may be used under the terms of the Creative Commons Attribution 3.0 licence. Any further distribution of this work must maintain attribution to the author(s) and the title of the work, journal citation and DOI.
Published under licence by IOP Publishing Ltd

the effect of flexural, shear and torsion loads [9]. Shear behavior of reinforced self-compacting concrete deep box beams strengthened internally by transverse ribs, also studied [10]. Furthermore, the effect of transverse internal ribs on shear strength evaluation of hollow RC beams was studied [11] Strengthening of continuous SCC hollow beams under shear stresses using warped CFRP strips were studied experimentally [12].

Despite that many investigation on the shear behavior of RC T-beams with solid or box cross-section, little has been done on the applications of SCC with a complete absent for effect of variation of hollowness ratio of box T-beams on structural performance. So the need to study the shear behavior of such sections with strengthening by CFRP technique gives more attention.

2. Experimental work Program

2.1. Beam Specimens Description

Eight simply supported beam specimens were tested under monotonically concentrated load at mid-span, to study the shear behavior of SCC box T-beams. The tested beams were designed in accordance with ACI 318-M14 Code [8] with minimum shear reinforcement to ensure that the beams will fail in a shear mode of failure. Three variables were adopted in the present study, section type (box or solid), thinned wall web thickness (50mm, 62.5mm, and 75mm) and with or without strengthening by CFRP. The beam specimens were (1500mm) long and were tested over an effective span of (1400mm). Designations and descriptions of tested beams are shown in table 1. The cross-section and longitudinal details of the test specimens are shown in figures 1 and 2.

Table 1. Beam specimens details.

Beam Designation	Beam Type	b_f (mm)	t_f (mm)	t_w (mm)	H (mm)	HR[b]	Strengthening
B1[a]	Box	400	50	2x50	300	27	None
B2	Box	400	50	2x50	300	27	CFRP
B3	Box	400	50	2x62.5	300	20.3	None
B4	Box	400	50	2x62.5	300	20.3	CFRP
B5	Box	400	50	2x75	300	13.53	None
B6	Box	400	50	2x75	300	13.53	CFRP
B7	Solid	400	50	200	300	-	None
B8	Solid	400	50	200	300	-	CFRP

[a]Reference Beam
[b] Ratio of hollow to the total cross sectional area

The main longitudinal reinforcement consisted of (4ϕ16mm) hot rolled, mild steel bars which work as tension reinforcement. Longitudinal tension reinforcement had 90-degree hooks at the beam ends with (160mm) long to ensure appropriate anchorage. Also (4ϕ6mm) deformed steel bars were used as holding bars at the top to hold the transverse reinforcement in position while the concrete was being poured. The beams were reinforced with minimum shear reinforcement, (ϕ6mm) at (130mm) c/c deformed bars were used as transverse reinforcement (stirrups). There is additional transverse reinforcement at the flange, (ϕ6mm) at (130mm) c/c deformed bars arranged between the spacing of stirrups. Both longitudinal and vertical bars were settled and connected together through using of (1mm) steel wires to form the reinforcement cage. The reinforcement mesh has been placed inside the mold with (18mm) concrete cover for tensile reinforcement and (10mm) from the top. Wooden molds with (18mm) thickness plywood were used to cast beam specimens. Each mold consists of a bed and two movable sides, these sides have been fixed together by screws to form the required shape. Polystyrene blocks are used to form the hollows inside the beams because it is lightweight and its facility to configure with the required dimensions. For all tested beams, beyond the cells (at the ends), the whole beam section was solid concrete.

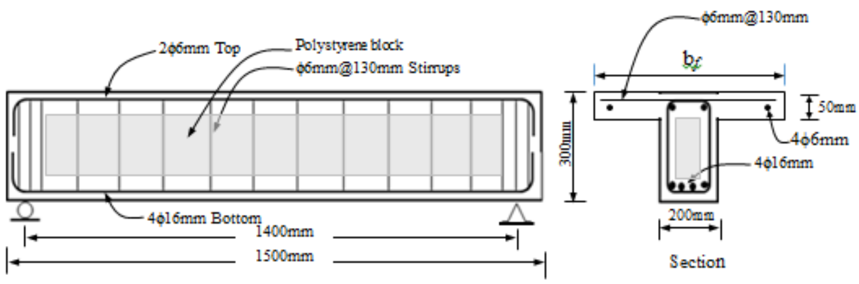

Figure 1. Box T-shaped beam specimen details.

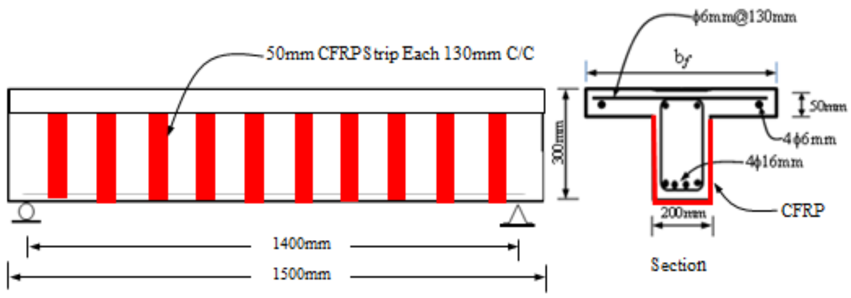

Figure 2. Strengthening of T-shaped beams by CFRP.

2.2. Materials

In manufacturing the test and control specimens, the following materials are used: ordinary Portland cement (Type I); natural sand with maximum size of (4.75mm) and fineness modulus of (3.18); crushed gravel with maximum size of (12mm); fine lime stone powder (L. S. P.) with fineness of (3100 cm^2/gm.), high water reducer superplasticizer (Glenium 51); clean tap water was used for both, mixing and curing. The concrete mix proportions were (400 kg/m^3), (797kg/m^3), (767kg/m^3), (170kg/m^3), (190$Liter/m^3$) and, (7.5$Liter/m^3$) for cement, sand, gravel, limestone, water and superplasticizer respectively. The reinforcement consists of (ϕ16 mm) deformed steel bars having yield strength of f_y= 491MPa and ultimate strength of f_u=653MPa were used as longitudinal reinforcement; while, for transverse reinforcement, (ϕ6 mm) deformed steel bars having yield strength of f_y= 473MPa and ultimate strength of f_u=651MPa were used.

2.3. Properties of Fresh and Hardened Concrete

For the fresh SCC, four tests to evaluate three characteristics (filling ability, segregation resistance, and passing ability) are made to check self-compacting concrete. Tests result shows that the adopted mix confirm the SCC requirements of EFNARC [13]. The compressive strength test has been carried out in accordance with ASTM C39/C39M-01[14] and BS 1881-116 1983 [15]. The compressive strength of the cylindrical specimens were (20.43MPa), (23.3MPa) and (28.7MPa) for (7days), (14days) and (28days) respectively. From the other wards, the compressive strength of the cubic specimens were (23.9MPa), (26MPa) and (34.5MPa) for (7days), (14days) and (28days) respectively. The indirect tensile strength was carried out according to ASTM C496-96 [16]. The value of (f_{ct}=2.95MPa) was measured for splitting tensile strength of concrete at the age of (28 days). Static modulus of elasticity was carried out according to ASTM C469-02 [17]. The value of (E_c =24750MPa) was measured for the modulus of elasticity of concrete at the age of (28 days).

2.4. Test Measurement and Instrumentation

The beams, as well as control specimens, were tested by using the universal hydraulic machine with maximum range capacity of (300ton). Vertical deflection was measured at two points, at the mid-span

IOP Conf. Series: Materials Science and Engineering **737** (2020) 012029 doi:10.1088/1757-899X/737/1/012029

and at one-third of the span of beam specimens by using dial gauge of (0.01mm/div.) accuracy at every load stage. The gauges were placed under the bottom face of the tested beams.

3. Numerical Analysis

3.1. Element Types and Beam Specimens Modeling

Three dimensional, nonlinear finite element analyses have been carried out in this study to analyze all experimentally tested beams. The analysis is performed by using finite element software ANSYS (Version-11). In ANSYS software, each element can be used to represent a specified constituent of beams [18]. A nonlinear, eight nodes brick element, (SOLID-65), with three translations DOF at each node, is used to model the concrete (SCC). By taking advantage of the symmetry of both, beam's geometry and loading, a quarter of the entire model beam was used for finite element analysis, figure 3a. For finite element modeling of the steel reinforcement (tensile, compressive, and stirrups), two nodes, discrete axial element, (LINK-8), with three translations DOF at each node is used. From the other hand, four nodes shell element, (SHELL-41), with three translations and three rotations DOF per node were used to model CFRP as shown in figure 3b**.** As in experimental work, the number of CFRP strips is ten vertical strips in the spacing between the shear reinforcement. Since the CFRP strips are created through the nodes of concrete elements full bond is considered between these two elements and no interface element is required to model the epoxy material. To avoid stress concentration, (10mm) thick steel plate is added at the load locations and modeled by using a nonlinear, eight nodes brick element, (SOLID-45), with three translations DOF (per node) in x, y, and z-directions. The externally load was applied on a steel plate across the entire centerline of the plate; thus, the external applied load was represented by the equivalent nodal forces on the top nodes of the same place of the plate. To certify that the model acts the same way as the experimental specimens, displacement boundary conditions are needed to constrain the model to get a good solution. The roller support is obtained by constraining nodes in a steel plate in the bottom of the beam in the y-z-directions ($U_y= U_z =0$).

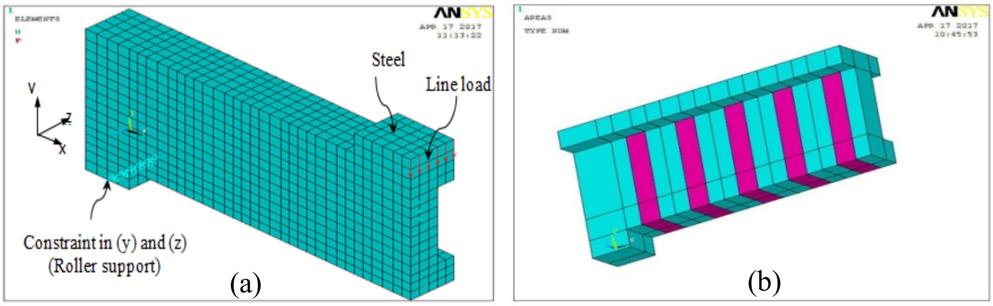

Figure 3. (a) Beam modeling, meshing and boundary conditions (b) CFRP strips modeling.

3.2. Parametric Study

The parametric study presented consists of analyzing sixteen additional beams which have been modeled using ANSYS software. The considered parameters in this numerical study include the compressive strength of concrete (*fc*'), use a high strength concrete with (50MPa) compressive strength and the presence of prestressing (strengthening the beams with two prestressed strands passing through the center of gravity of each beam). The prestressed beams have the same properties of non-prestressed experimentally tested beams also; the properties of the other materials were kept constant as in table 2.

3.2.1. Concrete Properties. A high strength concrete with (*fc'*=50 MPa) is used instead of normal strength SCC. The ultimate tensile strength of (*ft* =4.38MPa) and Young's modulus of Elasticity of (Ec=25323MPa) were calculated based on ACI 318-M14 code [8]. The open shear transfer coefficient (βo), closed shear transfer coefficient (βc) and Poisson's ratio (υ) were assumed as (0.3), (0.8) and

(0.2), respectively. The strain-stress relationship for concrete was created based on the equations of reference [19].

3.2.2. Prestressed Concrete Model. The prestressing strands were represented by using 2-node discrete representation (LINK-8 in ANSYS) and included within the properties of 8-node concrete elements (SOLID-65). The link element for the strand was connected between nodes of each adjacent concrete solid element, which mean perfect bond between strand and concrete, so the prestressing type is pre-tensioned. Each modeled beam was prestressed using two (12.5mm) diameter, (1800MPa) 7-wire strands. The location of strands was in the center of gravity of each beam, so the prestressed beam model would have subjected to initial axial compression stress only. The initial prestressing force is assumed to be equal to ($0.7f_{pu}$) as recommended by the equations of ACI 318-M14 [8] and the total losses (lumped sum losses) were assumed to be equal to (20%) as recommended by Nilson, A. H. [20]. Therefore, the initial prestressing force, effective prestressing force and initial strain value can be calculated directly as shown in table 2. It may be noted that, in ANSYS software, the prestressing effect is defined through the real constants by the initial strain value.

Table 2. Properties of prestressing strand for finite element models.

Parameter	Description	Value
A_{ps}	Cross section area (mm^2)	100.2
f_{pu}	Ultimate tensile strength of prestressed strand (MPa)	1800
f_{pi}	Initial prestressing (MPa)	1260
P_i	Initial prestressing force (kN)	126.25
P_e	Effective prestressing force (kN)	100
f_{pe}	Effective prestressing (MPa)	1000
ε_i	Initial strain	0.005
$E_s{}^a$	Modulus of elasticity (MPa)	$2x10^5$

[a] ACI 318-M14 [8]

4. Results and Discussion

4.1. Ultimate Load

Table 3, shows the comparison between the ultimate loads of the experimental (tested) beams, $(P_u)_{EXP.}$, final loads from the finite element models, $(P_u)_{FEM}$ and by using ACI-318-M14[8] design equations. The final loads for the finite element models are the last applied load steps before the solution starts to diverge due to numerous cracks and large deflections. In comparison with the reference beam (B1), which has 50mm wall web thickness, the ultimate load capacity increase about (17%, 16.5%, 38%) when the wall thickness has been increased from (50mm) to (62.5mm, 75mm, and became a solid). Each non-strengthened beam has a strengthened counterpart beam with same amount and distribution of CFRP, the presence of this strengthening increases the ultimate load capacity about (75%, 85%, 97%, and 110%) for wall web thickness of (50mm, 62.5mm, 75mm and became a solid) respectively. It is shown that increase in the walled web thickness gives higher shear capacity because the area of concrete on the web of a T-beam can provide an additional area for the compression zone, so the average stress at failure can be reduced and the shear capacity can be improved. Comparing with the experimental results, all the finite element models show relatively large capacity at the ultimate stage. It can be observed that there is a simulation between the finite element analysis and the experimental results of about (102%) for ultimate load capacity (P_u) and these ratios are considered reasonable and accepted. On the other hand, the application of the ACI-318-M14 design equations leads to an underestimation of the ultimate loads, this may be due to that the ACI-318-M14 code neglect the contribution of T-beam flange which provide a certain level of shear resistance above a certain width.

Table 3. Experimental and numerical results.

Beam	$(P_u)_{Exp.}$ (kN)	$(P_u)_{FEM}$ (kN)	$(P_u)_{ACI}$ (kN)	$(Pu_r)Exp. /(Pu_i)Exp.$	$(P_u)_{FEM} /(P_u)_{Exp}$	$(P_u)_{ACI} /(P_u)_{Exp}$	$(\Delta_u)_{Exp.}$ (mm)	$(\Delta_u)_{FEM}$ (mm)	Failure Mode
B1	206	195	145	-	0.95	0.70	3.2	2.8	D/Tension
B2	360	380	-	1.750	1.06	-	3.5	3.2	Debonding
B3	230	228	157	1.170	0.99	0.68	3.5	3.1	D/Tension
B4	382	391	-	1.850	1.02	-	3.2	2.9	Debonding
B5	240	245	169	1.165	1.02	0.70	4.0	3.5	D/Tension
B6	405	417	-	1.970	1.03	-	3.7	3.3	Debonding
B7	283.5	290	193	1.380	1.02	0.68	4.3	3.7	D/Tension
B8	435	455	-	2.110	1.05	-	4.5	3.6	Debonding

4.2. Load versus Deflection Curves

Load-deflection curves at mid-span at all stages of loading up to failure are plotted and presented in figure 4a. Each curve initiated in a linear form with a constant slope, change to a nonlinear form with a varying slope. Then, the third stage starts when the deflection increases very fast with a small increase in the applied load. The increase of wall web thickness exhibits an increase in load carrying capacity and this is reflected in the corresponding deflections, this is due to that the moment of inertia and stiffness of beams increase with the increasing of web thickness. At a certain load level, the reference beam has lower deflection values; this may be due to the influence of moment of inertia where it increased as the wall web thickness increase as well as the stiffness. In each curve, it is noted that the beams which strengthened with CFRP strips continued in carrying the load for about twice the loading capacity of beams without strengthening and this is reflected in the corresponding deflections. The presence of CFRP strips increase load carrying capacity, as a result, the toughness (area under load-deflection curve) of the beams increased, so the absorption of deformations was increased.

The load versus deflection curves obtained from the finite element analysis together with the experimental tests are plotted and presented in figure 4b. In general, it can be noted from the load-deflection curves that the finite element analyses agree well with the experimental results throughout the entire range of behavior**.** The simulation between the finite element analysis and the experimental results of about (85%) for ultimate deflection (Δu) and these ratios are considered reasonable and accepted.

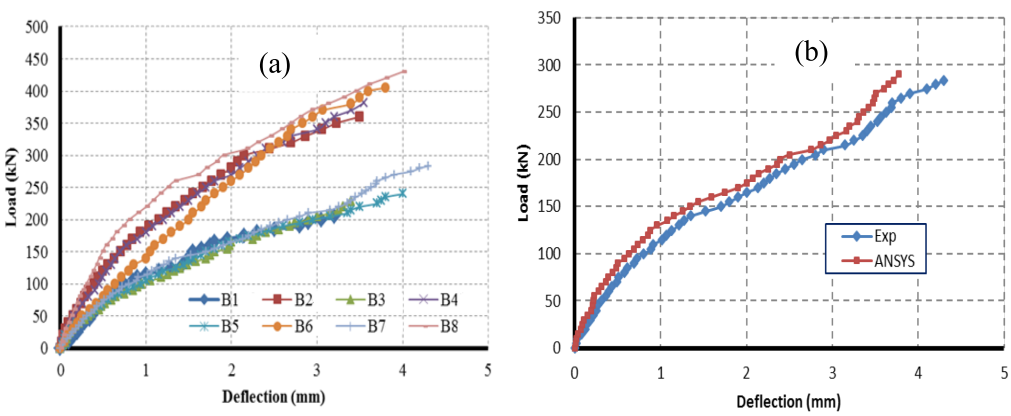

Figure 4. (a) Load-Deflection curves for tested beams (b) for beam specimens B7

4.3. Crack Patterns

As the load increased, the first diagonal crack (web shear crack) appears at the mid-height of the diagonal region bounded by load and support positions in both shear spans at the same load level or little different and then extended upward toward the load point, then these inclined cracks multiplied and became wider in shear spans. One or more cracks propagated faster than the others and reached the top flange (near the applied load where crushing of the concrete near the positions of applied loads had occurred due to highly concentrated stresses under the point load) and nearly horizontally at the level of the longitudinal reinforcement toward the support in the other direction. The top flange was cracked in longitudinal and transverse axes. The failure occurs by splitting the beam into two parts approximately along the line joining the edge steel blocks at the support and point of loading where the loaded part drop by some millimeters away from another part. This mode of failure can be considered as a "Diagonal Tension Failure". In strengthened beams, the failure modes were either CFRP debonding or CFRP rupture as shown in figure 5.

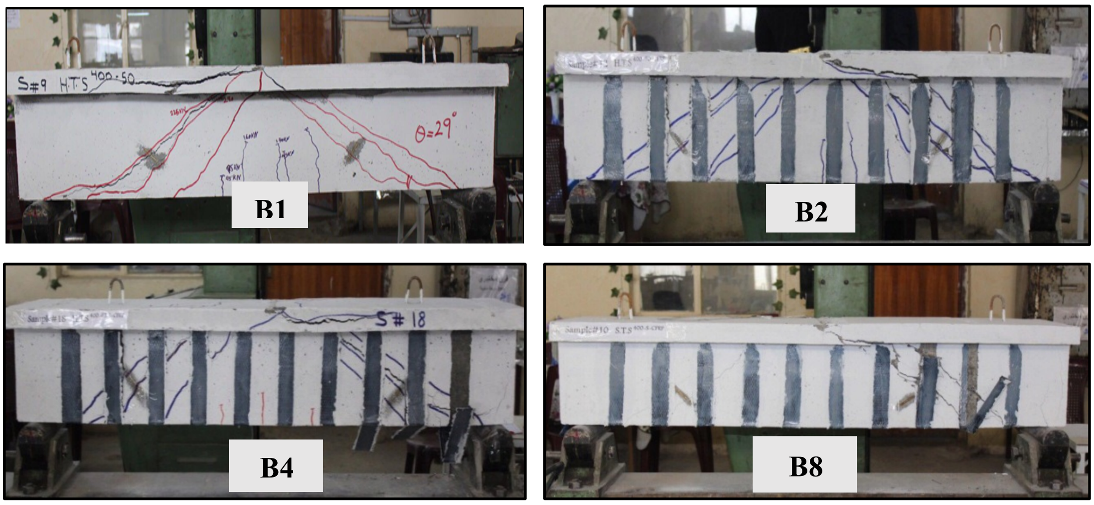

Figure 5. Crack patterns for tested beams.

The ANSYS program records the crack pattern at each applied load step. There is a good agreement between the finite element analysis and the experimental response for the beams crack patterns as shown in figure 7. The appearance of the cracks reflects the failure mode for the beams. The model of FEM, accurately, predicts that the tested beams are failing in shear and predicts that the vertical and inclined cracks formed in the shear span regions respectively. The cracks are concentrated in the shear span region and vanish diagonally towards the beam supports.

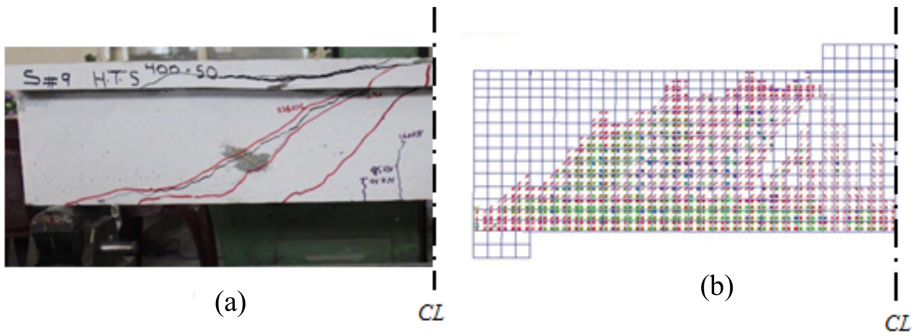

Figure 6. Crack patterns (a) experimental testes (b) finite element model

IOP Conf. Series: Materials Science and Engineering **737** (2020) 012029 doi:10.1088/1757-899X/737/1/012029

4.4. Parametric Study Analysis Results

Parametric study analysis results are reported and given in table 4. There is no doubt that increasing compressive strength of concrete causes an increase in ultimate tensile strength of concrete which has a main effect on the inclined cracking load (shear failure). It can be noticed that, when the value of (f'c) increases, the value of ultimate capacity (Pu) and the deflection (Δf) increase too. More specifically, the increase in (*fc'*) value from (28.7 MPa) to (50 MPa) led to increase in ultimate load capacity about (17%, 11%, 14% and 12%) for beams with webs thickness (50mm, 62.5mm, 75mm and solid) respectively and about (8%, 9%, 6% and 8%) for beams that have strengthened by CFRP with same above arrangement for webs thickness.

Table 4. Ultimate load capacity of numerically analyzed models[a].

Beam Designation	Pu (kN)	Increasing in Pu %	Beam Designation	Pu (kN)	Increasing in Pu %	Beam Designation	Pu (kN)	Increasing in Pu %
B1	195	-	H-B1	228	17	PH-B1	350	79
B2	380	-	H-B2	410	8.0	PH-B2	635	67
B3	228	-	H-B3	254	11	PH-B3	415	82
B4	391	-	H-B4	425	9.0	PH-B4	668	71
B5	245	-	H-B5	280	14	PH-B5	435	78
B6	417	-	H-B6	440	6.0	PH-B6	705	69
B7	290	-	H-B7	326	12	PH-B7	522	80
B8	455	-	H-B8	490	8.0	PH-B8	731	61

[a]The comparision is done with respect of corresponding model (Experimental Specimens, modeled by ANSYS)
[b](H) symbol means using a high strength concrete (*fc'=50* MPa*)*.
[c](PH) symbol means presence of prestressing and using (*fc'=50* MPa)

The presence of the prestressing force led to increase the ultimate load capacity and delay the initiation of cracks. Strengthening the beams with (*fc'=50* MPa) with two (12.7mm) diameter (1860 MPa) 7-wire strands make increasing in ultimate load capacity about (79%, 82%, 78%, and 80 %) for T-beams with webs thickness of (50mm, 62.5mm, 75mm, and solid) respectively. While the ultimate load capacity for beams that have to strengthen with CFRP strips increased about (67%, 71%, 69%, and 61%), respectively. Figure 7 shows the effect of parametric study variables on crack pattern for modeled beam (B7). It can be noted that the presence of prestressing led to decrease the amount of cracks.

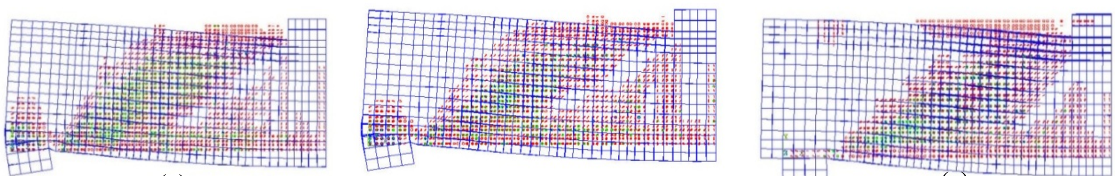

(a) (b) (c)

Figure 7. (a) Crack pattern for modeled Beam B7, (b) After Increasing of Compressive Strength (H-B7), (c) After Increasing of Compressive Strength with Prestressing (PH-B7)

5. Conclusions

The mechanism of failure of reinforced concrete beams was investigated well by using the adopted finite element models. The ultimate loads predicted were very close to the ultimate loads measured in experimental tests. It can be observed that there is a simulation between the finite element analysis and the experimental results of about (102%) for ultimate load capacity (P_u) and this ratio is considered reasonable and accepted. The general behavior of the finite element models, represented by the load-deflection plots at mid-span shows good agreement with the test data from the experimentally tested beams**.** The crack patterns at the final loads from the finite element models compared well with the observed failure modes of the experimental beams. Analysis results of the parametric study show that the increase of concrete compressive strength (f_c') from (28.7MPa) to (50MPa) leads to increase in ultimate load capacity about (11-17%)*,* while the ultimate load capacity increased for about (78-82%) when the beams were prestressed.

Acknowledgements
The authors wish to express thanks and appreciation to the Engineering staff of the civil Engineering Department, College of Engineering, Mustansiriyah University.

References
[1] Lars J R 1996 Plastic Behavior of Deformable Reinforced Concrete Box Sections Under Eccentric Load Ph.D. Thesis, University of Queensland
[2] Al-Janabi W A 2005 Analysis and Shape Optimization of Varied Section Box Girder Bridges M.Sc. Thesis, University of Tikrit, Iraq.
[3] Aziz A H and Jasem M A 2017 CFRP Shear Strengthening Performance of Varying Hollowness Ratio Reinforced Self Compacting Concrete Box T-Beams *IJCSEIERD* **7** pp 55-70
[4] Taljsten B 2003 Strengthening Concrete Beams for Shear with CFRP Sheets *Construction and Building Materials* **17** pp 15-26
[5] Neale K W, 2000 FRPs for Structural Rehabilitation: A Survey of Recent Progress *Progress in Structural Engineering and Materials* **2** pp 133-38
[6] Aziz A H, Yousif M Z and Salman L K 2012 Experimental Evaluation of effect of flange dimensions on Shear Behavior of NSC and SCC Double Tee Beams *Engineering and Technology Journal* **30** pp 3039-53
[7] Aziz A H, Mahdi H A and Abd Al-Hussein A J 2012 Experimental Evaluation of Shear Strength of RPC T-Beams with Smooth or Rough Construction Joints *Engineering and Development Journal, Refereed Scientific Engineering Journal (Special issue)* **1** pp 317-34
[8] ACI 318M-14, 2014 Building Code Requirements for Structural Concrete (ACI 318-M14) *ACI, USA*.
[9] Chiad S S, 2013 Shear Stresses of Hollow Concrete Beams *Journal of Applied Sciences Research* **9** pp 2880-89
[10] Hassan R Y 2015 Evaluation of Shear Strength of RC deep box beams strengthened internally by Transverse Internal Ribs MSc Thesis, Al-Mustansiriyah University, Iraq.
[11] Aziz A H 2016 Effect of Transverse Internal Ribs on Shear Strength Evaluation of Hollow RC Beams *Journal of Engineering* **22** pp 11-25
[12] Aziz A H, Alfeehan A A and Hussein F A 2016 Strengthening of Continuous SCC Hollow Beams under Shear Stresses using warped CFRP Strips *Civil and Environmental Research* **8** pp 105-16
[13] EFNARC, 2002 Specification and Guidelines for Self-Compacting Concrete Association House, 99 West Street, Farnham, Surrey GU9 7EN, UK, Available at (www.efnarc.org).
[14] ASTM C39-96, 1996 Test Method for Compressive Strength of Cylindrical Concrete Specimens ASTM, USA.
[15] BS 1881-116, 1983 Method for Determination of Compressive Strength of Concrete Cubes BSI, London, UK.
[16] ASTM C496-96, 1996 Standard Test Method for Splitting Tensile Strength of Cylindrical Concrete Specimens ASTM, USA.
[17] ASTM C 469-02, 2002 Standard Test Method for Static Modulus of Elasticity and Poisson's Ratio of Concrete in Compression *ASTM, USA*.
[18] ANSYS Manual, Version (11).
[19] Desayi P and Krishnan S 1964 Equation for the Stress-Strain Curve of Concrete *J. ACI* **61** pp 345-50.

IOP Conf. Series: Materials Science and Engineering **737** (2020) 012029 doi:10.1088/1757-899X/737/1/012029

[20] Nilson A H 1983 *Design of Prestressed Concrete* 2nd Edition, New York, USA, John Wiley & Sons Inc.